Fractional Quantum Hall States in a Ge Quantum Well

O. A. Mironov[1,2], N. d'Ambrumenil[1], A. Dobbie[1], A. V. Suslov[3], E. Green[4] and D. R. Leadley[1]
[1]*Department of Physics, University of Warwick, Coventry CV4 7AL, UK*
[2]*International Laboratory of High Magnetic Fields and Low Temperatures, Wroclaw, Poland*
[3]*National High Magnetic Field Laboratory, 1800 East Paul Dirac Drive, Tallahassee, FL 32310, USA*
[4]*Hochfeld-Magnetlabor Dresden (HLD-EMFL), Helmholtz-Zentrum Dresden-Rossendorf, D-01314 Dresden, Germany*
(Dated: May 23, 2016)

Measurements of the Hall and dissipative conductivity of a strained Ge quantum well on a SiGe/(001)Si substrate in the quantum Hall regime are reported. We analyse the results in terms of thermally activated quantum tunneling of carriers from one internal edge state to another across saddle points in the long range impurity potential. This shows that the gaps for different filling fractions closely follow the dependence predicted by theory. We also find that the estimates of the separation of the edge states at the saddle are in line with the expectations of an electrostatic model in the lowest spin-polarised Landau level (LL), but not in the spin-reversed LL where the density of quasiparticle states is not high enough to accommodate the carriers required.

PACS numbers: 73.20.Mf, 73.21.-b, 73.40.Hm, 73.43.Cd, 73.43.Lp

arXiv:1512.06985v2 [cond-mat.str-el] 20 May 2016

The strongest fractional quantum states have been found in delta-doped GaAs quantum wells and heterostructures. These have been the cleanest samples with the highest mobilities and yet the strength of a fractional quantum Hall state does not appear to be connected in a simple way with the zero magnetic field mobility of the samples involved [1, 2].

The strength of a quantum Hall state is associated with how rapidly the dissipative conductance drops with temperature. This is known to be affected by the long-range impurity potential, arising out of the ionised donors in a semiconductor heterostructure, although describing this effect quantitatively has proved difficult. The background potential leads to the formation of compressible regions, which then partially screen the background potential. Predicted theoretically in [3, 4], and later verified in scanning electron transistor measurements [5], these compressible regions are separated from the percolating incompressible region by internal edges. The transfer between these internal edges is then the principal dissipative process at low temperatures [6, 7]. Characterising these internal edges is not just an important challenge for describing the quantum Hall response, but also to the interpretation of Aharonov-Bohm interference experiments at filling factor $\nu = 5/2$ [8]. It turns out, for example, that it is crucial to the interpretation of these experiments to know whether any charge redistribution associated with changing the field occurs internally (by shifts in the local occupation of compressible regions) or by the outer sample edges [9].

Here, we report conductivity measurements on a p-type strained germanium quantum well. There is a clear family of quantum Hall states in the composite fermion (CF) series centered on $\nu = 1/2$ [10]. Our analysis of the data shows that the model can give a consistent fit across all filling fractions in the CF family for the gaps in these systems and explains why the zero field mobility is not simply connected with the strength of the quantized Hall states. The gaps are in line with the predicted dependence on filling fraction. In addition we estimate the typical separation at a saddle point, a, of two compressible regions occupied by the same type of carrier. As a function of the gap, these correlate well with the separation of neighboring compressible regions containing carriers of opposite charge, which can be predicted on the basis of an electrostatic model [11]. While the dependence of the width parameter, a, on the gap, Δ_s, is the same for filling fractions in the lowest Landau level (LL) above and below $\nu = 1/2$, there is a systematic shift to higher values for the quasihole states ($\nu > 1/2$). However, for states above $\nu > 1$ where multiple LLs are occupied, the dependence does not coincide with the predictions of the electrostatic model. We attribute this to the need for a charge rearrangement across the incompressible region, which is too large for a simple edge to accommodate.

Our sample was grown by reduced pressure chemical vapour deposition at the University of Warwick (sample ID 11-289SQ1D). It is taken from the same wafer that was reported in [12], it has a density of 2.9×10^{11} cm^{-2} and a mobility of 1.3×10^6 cm^2/Vs (with current flow along the [110] direction). The hole effective mass of $0.073(1)m_e$, measured from the temperature dependence of the Shubnikov-de Haas oscillations at low field, is remarkably similar to that of electrons in GaAs ($0.067m_e$) and much lower than for holes in GaAs. The Dingle ratio is 78 ± 2 [13, 14].

Fig. 1 shows the structure of the wafer. A reverse linear graded, strain tuning buffer [15] terminating in over-relaxed $Si_{0.2}Ge_{0.8}$, is followed by the Ge quantum well which is under 0.65% biaxial compressive strain. Holes are supplied from a boron doped layer that is set back 26 nm above the quantum well. Magnetoresistance measurements were performed at the National High Magnetic Field Laboratory using static fields of up to 35 T and at temperatures down to 26 mK. We note that results on

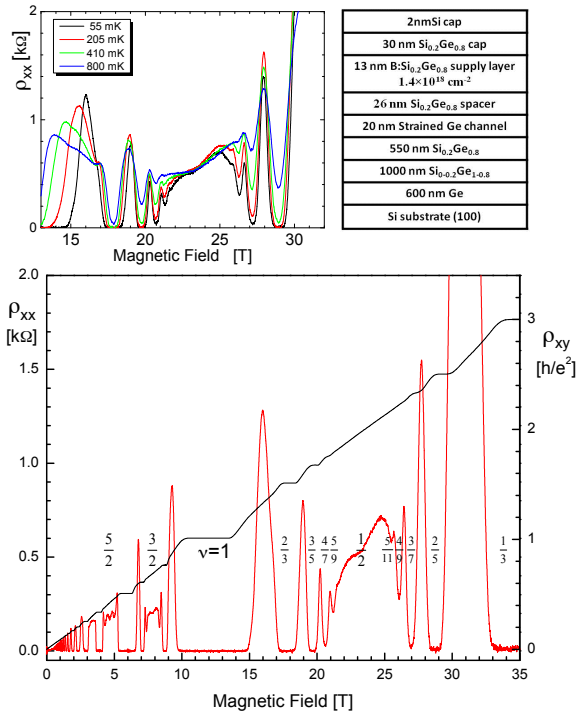

Figure 1. The Hall resistance, ρ_{xy}, and dissipative response, ρ_{xx}, at 55mK (main figure) and the dissipative response at different temperatures [14] in the high field regime (top left). The wafer structure is summarized in the schematic (top right).

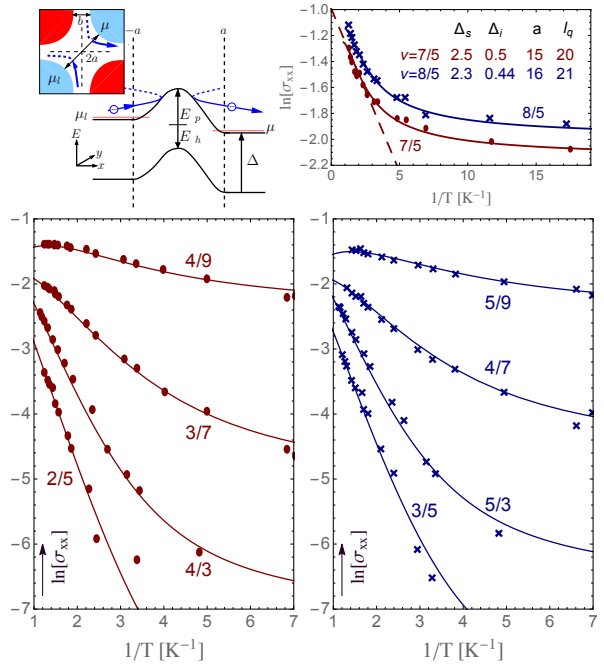

Figure 2. Band alignment and particle flow across a typical saddle point in the potential (top left). The blue/red regions are compressible with nucleated QPs/QHs, while the white region is incompressible. Dissipation occurs when excitations move across a saddle point from a compressible region with chemical potential, μ_l, to compressible region at μ_r. The transfer proceeds by thermally activated tunneling across the energy barrier, which on average is $\Delta_s/2$. The resulting logarithmic conductance (with σ in units of $2(qe^2)/h$) at different filling fractions is shown top right and below. For the $\nu = 7/5$ and $\nu = 8/5$ states, the theoretical prediction and model parameters used to describe the data are shown (the data at $\nu = 8/5$ have all been raised by 0.1 for clarity).

a similar sample grown in our laboratory have already been reported [16] but without any discussion of the CF family in the lowest Landau level.

Figure 1 shows field-traces of the longitudinal resistance taken in a 4×4 mm square geometry at four different temperatures with the current along the [110] direction. The Hall resistance was measured separately in a Hall bar geometry. There are clear quantum Hall states at fractions in the main CF sequence around $\nu = 1/2$ and $\nu = 3/2$. As seen in CdTe [17], there is some deviation from simple activated behavior even when there are good quantum Hall states. Around $\nu = 5/2$ we find a minimum on ρ_{xx} but no clear plateau at $\nu = 5/2$. The mobility of our sample is high for a Ge sample, but it is still significantly less than for GaAs samples showing such clear FQH states. For example in a p-doped GaAs sample, with $\mu = 2.3 \times 10^6$ cm^2/Vs (close to twice that of our sample), there are precursor signals of states at $\nu = 3/5$ and at $\nu = 4/7$ but not quantized Hall states [18]. In n-doped GaAs no sign of the $\nu = 5/2$ state is visible for $\mu \lesssim 6.7 \times 10^6$ cm^2/Vs [1, 2].

While the zero field mobility reflects all scattering, we assume that it is the long-range potential of the ionized donors that controls the dissipation in quantum Hall states. Any short range scattering centres, not located directly in the saddle points of the long range impurity potential, will not affect the response of the quantum Hall state. This makes clear why mobility is unlikely to be a good indicator of strong quantum Hall states [1].

We have analysed the data using the model developed in [7, 19]. This assumes that localized regions or puddles of compressible regions are nucleated within the incompressible quantum Hall fluid. The dissipative response is controlled by excitations, localized in one puddle, crossing to another via a saddle point in the impurity potential, see Fig. 2. The saddle points act as effective resistors and the puddles of quasiparticles (QP) and quasiholes (QH) act as reservoirs in a resistor network [6]. The response is then that of the average saddle point (with barrier height $\Delta_s/2$) [20, 21].

If the energy required to create a QP/QH pair near a saddle is Δ_s, the average barrier height to traverse a saddle is $\Delta_s/2$ for both QPs (E_{sp}) and QHs (E_{sh}). In the absence of tunneling through the saddle point, the dissi-

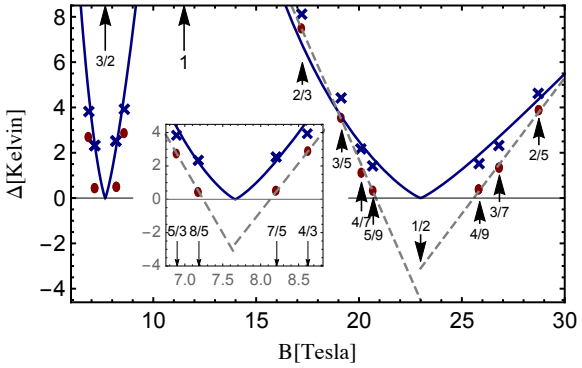

Figure 3. Estimates of the gap as a function of magnetic field. The crosses denote the estimate of the gap at each ν, Δ_s. The ovals show the energies, Δ_i, estimated from the gradients in the Arrhenius plots taken at the point of inflection for each ν (see Fig. 2) . The solid lines are the dependence predicted in CF theory [23] with $C' = 2$ and $C = 0.25$, see (2). The dashed straight lines are best linear fits. Insert: Results close to $\nu = 3/2$ on an expanded scale.

pative conductance per square is $[2(qe)^2/h]\, e^{-\Delta_s/2kT}$ as predicted by Polyakov and Shklovskii [6]. Taking account of tunneling gives a dissipative conductance per square

$$\sigma_{xx}^{\square} = 2\frac{(qe)^2}{h} F[\Delta_s, a/l_q], \tag{1}$$

where a is the typical saddle point width (see Fig. 2) and l_q is the magnetic length for QPs/QHs with fractional charge qe [7, 14, 22] . We fit the data to the computed form for F using the gap, Δ_s, and the width parameter, a, as free parameters.

We convert the measured minimum values of ρ_{xx} at each filling fraction and for each temperature to equivalent conductivities σ_{xx} (the Hall resistance is taken as the corresponding quantized value). The results for $\nu = 7/5$ are shown in Figure 2. We also show the results of the more traditional method of assuming the Arrhenius form, drawing a tangent to the curves at the inflection point and identifying the gradient with an energy gap, Δ_i.

The aspect ratio (width/length) of the active region of the sample gives an overall additive constant to $\ln \sigma_{xx}$ [14]. We use this as a consistency check on the model as it should not vary significantly between filling fractions. For the states at $\nu = 2/3, 2/5, 3/5, 3/7$ and $4/7$, the data in Fig. 2 fitted assuming a constant aspect ratio of 1.8. At filling fractions with small gaps, we can expect that the effective width of the percolating incompressible region may reduce as the state is weaker. At $\nu = 4/9$ and $\nu = 5/9$ the aspect ratio is reduced to 1.4 and 1.5 respectively. However, we should emphasize that at these filling fractions the states are weak (the ratio between low and high temperature conductance is less than 1.9).

In Fig. 3 we compare the results for Δ_s with the predicted dependence on magnetic field for the composite fermion model [23]. For spin-polarised states at filling fraction $\nu_p = p/(2p+1)$, $1 \pm \nu_p$ or $2 - \nu_p$, the theory predicts that the gap in a homogeneous system, Δ_h, varies as

$$\Delta_h = \frac{C}{|2p+1|(\ln|2p+1| + C')} \frac{e^2}{\epsilon l_0}, \tag{2}$$

where C and C' are dimensionless constants and l_0 is the magnetic length. Analysis of the logarithmic divergences as $p \to \infty$ for a homogeneous system with zero width and without LL-mixing corrections suggested $C = 1.27$ [23] while comparison with exact diagonalization studies put $C' = 3.0$ and, later, $C' = 4.11$ [24]. We have treated C and C' as free parameters and compared with the values we obtain for Δ_s. The results are shown as solid lines in Fig. 3 with $C = 0.25$ and $C' = 2$.

The agreement between CF theory and the estimated gaps, Δ_s, is good even at filling fractions above $\nu = 1$. The values of the constants C and C' are different from those estimated for the homogeneous zero width case and indicate a larger role for the logarithmic corrections to the CF effective mass. The result (2) can be rewritten as a formula for the effective mass via

$$m^*(p) = \hbar^2 \left(\frac{\epsilon l_0}{e^2}\right) \frac{\ln|2p+1| + C'}{C}. \tag{3}$$

As expected the effective mass depends on the magnetic length—it varies between 0.69 m_e at $\nu = 5/3$ to 1.09 m_e at $\nu = 2/3$ (both have $p = -2$) and on p. Our results also suggest that the dependence of the effective mass on p is stronger than predicted for the homogeneous 2DEG ($C' = 2$ instead of 4.1 suggested by diagonalizations of the Hamiltonian of homogeneous systems [24]).

Although there is no microscopic model giving the typical saddle point width, a, as a function of Δ_s, we assume that it should be related to b, the width of the incompressible region between two puddles (see upper left pane in Fig. 2). We estimate b using the theory developed for edges, which computes the electrostatic potential induced by fixing the charge density at the incompressible value [11]. The width, b, is determined by setting the energy to create a quasiparticle-quasihole (QP-QH) pair equal to the electrostatic energy gained by transferring a QP from the low to the high density side of the incompressible region. This gives $b^2 = \frac{8e(e/q)\Delta}{q\,\pi\, dn/dx|_c}$ where $dn/dx|_c$ is the gradient of the carrier density at the centre of the incompressible strip if the system were fully screening of the background impurity potential.

In Fig. 4(a) we show a as a function of $\sqrt{\Delta_s/q}$ where the Δ_s are values from fits to the data. For the two families $\nu^{qp} = p/(2p+1)$ and $\nu^{qh} = 1 - p/(2p+1)$, we see that a linear dependence on $\sqrt{\Delta_s/q}$ works quite well. There is evidence of a systematic difference between the QP family and the QH family, with the width in the QH case slightly larger than in the QP case. A difference between

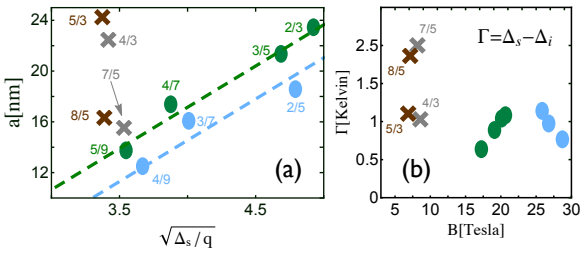

Figure 4. (a) The saddle point width parameter, a, plotted against $\sqrt{\Delta_s/q}$ (in units of $K^{1/2}$), for the different CF families (left). Dashed lines are guides to the eye. (b) $\Gamma = \Delta_s - \Delta_i$ for different filling fractions. Γ reflects the reduction in the apparent gap due to tunneling and has traditionally been assumed independent of filling factor.

the two cases is not surprising, given that the boundary of a compressible puddle is an internal edge and the fractionally charged QP/QH is an internal edge excitation. As the model does not factor in any details of the edge state reconstruction, a small systematic difference between the results for the two families ($\nu = p/(2p+1$ and $\nu = 1 - p/(2p+1)$) is to be expected.

In the case of the partially occupied reverse spin LL (RSLL), Fig. 4(a) shows that a does not follow the simple CSG scaling [11]. The scaling assumes that the compressible regions behave like perfect metals, *i.e.* that the screening length in the puddles is short enough for the electrostatic model to be a good approximation. This turns out to be unlikely in the RSLL in our sample. The theory would require that the screening electron density changes between edges of an incompressible strip by $\Delta n \sim b\, dn/dx|_c$. At filling fraction, $\nu = 1 + p/(p+1)$, the corresponding change in number density of QPs, with charge $qe = e/(2p+1)$, is $\Delta n_{QP} = \Delta n/q$. The average density of electrons in the RSLL is $n_1 = n\,p/(3p+1)$. This gives:

$$\frac{\Delta n_{QP}}{n_1} = \frac{\Delta n}{n}\frac{(2p+1)(3p+1)}{p}. \qquad (4)$$

For uncorrelated ionised donors, the typical density gradient would be $dn/dx|_c \sim \sqrt{n/8\pi}/d^2$ [4], which would give $\frac{\Delta n_{QP}}{n_1} \sim 0.2$ at $\nu = 4/3$ (p=1) and 0.3 at 8/5 (p=2). These would be large density variations in a LL and would take the system close to (or into) neighboring CF states (in the CF model, a ratio 1/(p+1) defines the next CF state in the hierarchy). The assumption of fully screening metallic regions, which is implicit in the CSG model, applies to this sample at filling fractions above $\nu = 1$.

Our model is not consistent with an approach, which assumes a $\nu-$independent broadening due to impurities. The difference, $\Gamma = \Delta_s - \Delta_i$, between the intrinsic gap and the slope measured in Arrhenius plots of the dissipative conductance, depends on the strength of the incompressible state. Fig 4(b) shows the broadening parameter, Γ, which, according to our model, varies between 2.5K at $\nu = 7/5$ and around 0.6K at $\nu = 2/3$. Γ is smaller the larger the intrinsic gap. On the other hand, the dashed lines in Fig. 3(a) show that, if we fit Δ_i by a linear function of $B - B(\nu = 1/2)$ [10], we obtain different values for the broadening and effective masses: 4.5K and $0.65m_e$ for $\nu < 1/2$, and 3.1K and $1.1m_e$ for $\nu > 1/2$. We conclude that estimates of intrinsic gaps using states of significantly different strengths on the basis of a $\nu-$independent broadening parameter are likely to be unreliable, see also [25].

We have reported measurements of the dissipative response and the Hall response of a Ge quantum well in the fractional quantum Hall regime. The results across all filling fractions, for which FQH states are found, fit well with the predictions of a model of thermally assisted quantum tunneling. The model demonstrates that the properties of the internal edge states around puddles control how a fractional quantum Hall state responds to any slowly varying background potential. Our sample has a high mobility for Ge but still significantly below that for GaAs samples (both p- and n-type) but shows much stronger quantum Hall states than would be expected given the mobility. Our model makes clear why the mobility is not likely to be a reliable measure of the sample in the quantum Hall regime. The strength of the quantum Hall state is determined by the strength of the long-range impurity potential at saddle points in the potential.

We thank R. H. Morf, R. Morris and M. Myronov for helpful discussions. We acknowledge support from EPSRC grants EP/J001074 and EP/F031408/1. The National High Magnetic Field Laboratory is supported by NSF Cooperative Agreement No. DMR-1157490 and by the State of Florida. We thank G. Jones, S. Hannahs, T. Murphy, J.-H. Park, and M. Zudov for technical assistance with experiments at NHMFL. OAM thanks M.Uhlarz, M. Helm and J. Wosnitza for the support of the initial HLD-HZDR 25 mK/16T measurements in 2012 and the National Scholarship Program of the Slovak Republic for the Researchers Mobility Support in 2013.

[1] N. Deng, G. C. Gardner, S. Mondal, E. Kleinbaum, M. J. Manfra, and G. A. Csáthy, Phys. Rev. Lett. **112**, 116804 (2014).
[2] V. Umansky, M. Heiblum, Y. Levinson, J. Smet, J. Nuebler, and M. Dolev, Journal of Crystal Growth **311**, 1658 (2009).
[3] A. L. Efros, Solid State Comm. **67**, 1019 (1988).
[4] F. G. Pikus and A. L. Efros, Phys. Rev. B **47**, 16395 (1993).
[5] J. Martin, S. Ilani, B. Verdene, J. Smet, V. Umansky, D. Mahalu, D. Schuh, G. Abstreiter, and A. Yacoby, Science **305**, 980 (2005).
[6] D. G. Polyakov and B. I. Shklovskii, Phys. Rev. Lett. **73**,

1150 (1994).
[7] N. d'Ambrumenil, B. I. Halperin, and R. H. Morf, Phys. Rev. Lett. **106**, 126804 (2011).
[8] R. L. Willett, C. Nayak, K. Shtengel, L. N. Pfeiffer, and K. W. West, Phys. Rev. Lett. **111**, 186401 (2013).
[9] C. W. von Keyserlingk, S. H. Simon, and B. Rosenow, Phys. Rev. Lett. **115**, 126807 (2015).
[10] J. K. Jain, Phys. Rev. Lett. **63**, 199 (1989).
[11] D. B. Chklovskii, B. I. Shklovskii, and L. I. Glazman, Phys. Rev. B **46**, 4026 (1992).
[12] A. Dobbie, M. Myronov, R. J. H. Morris, A. H. A. Hassan, M. J. Prest, V. A. Shah, E. H. C. Parker, T. E. Whall, and D. R. Leadley, Appl. Phys. Lett. **101**, 172108 (2012).
[13] O. A. Mironov, A. H. A. Hassan, M. Uhlarz, S. Kiatgamolchai, A. Dobbie, R. J. H. Morris, J. E. Halpin, S. D. Rhead, P. Allred, M. Myronov, S. Gabani, I. B. Berkutov, and D. R. Leadley, Phys. Status Solidi C **11**, 61 (2014).
[14] See Supplemental Material for details of the thermometry, sample characterization and theoretical background.
[15] V. A. Shah, A. Dobbie, M. Myronov, D. J. F. Fulgoni, L. J. Nash, and D. R. Leadley, Appl. Phys. Lett. **93**, 192103 (2008).
[16] Q. Shi, M. A. Zudov, C. Morrison, and M. Myronov, Phys. Rev. B **91**, 241303 (2015).
[17] B. A. Piot, J. Kunc, M. Potemski, D. K. Maude, C. Betthausen, A. Vogl, D. Weiss, G. Karczewski, and T. Wojtowicz, Phys. Rev. B **82**, 081307 (2010).
[18] J. D. Watson, S. Mondal, G. Gardner, G. A. Csáthy, and M. J. Manfra, Phys. Rev. B **85**, 165301 (2012).
[19] N. d'Ambrumenil and R. H. Morf, Phys. Rev. Lett. **111**, 136805 (2013).
[20] A. M. Dykhne, Sov. Phys. JETP **32**, 63 (1971).
[21] P. Asman, Unpublished, University of Warwick, (2015).
[22] H. A. Fertig and B. I. Halperin, Phys. Rev. B **36**, 7969 (1987).
[23] B. I. Halperin, P. A. Lee, and N. Read, Phys. Rev. B **47**, 7312 (1993).
[24] R. H. Morf, N. d'Ambrumenil, and S. Das Sarma, Phys. Rev. B **66**, 075408 (2002).
[25] N. Samkharadze, J. D. Watson, G. Gardner, M. J. Manfra, L. N. Pfeiffer, K. W. West, and G. A. Csáthy, Phys. Rev. B **84**, 121305 (2011).

Fractional Quantum Hall States in a Ge Quantum Well—Supplementary Information

O. A. Mironov[1,2], N. d'Ambrumenil[1], A. Dobbie[1], A. V. Suslov[3], E. Green[4] and D. R. Leadley[1]
[1]*Department of Physics, University of Warwick, Coventry CV4 7AL, UK*
[2]*International Laboratory of High Magnetic Fields and Low Temperatures, Wroclaw, Poland*
[3]*National High Magnetic Field Laboratory, 1800 East Paul Dirac Drive, Tallahassee, FL 32310, USA*
[4]*Hochfeld-Magnetlabor Dresden (HLD-EMFL), Helmholtz-Zentrum Dresden-Rossendorf, D-01314 Dresden, Germany*

arXiv:1512.06985v2 [cond-mat.str-el] 20 May 2016

In resistivity measurements in the quantum Hall regime, it is crucial to be able to have confidence in the measurement of the temperature. We used a RuO temperature sensor, which was mounted on the probe near the sample. Both sample and thermometer were loaded directly into the mixing chamber and thus were immersed in the mixture, in order to secure equal temperatures for the sample and thermometer.

To avoid sample self-heating low current measurements of 20 nA and 50 nA were used. As only the zero field calibration curve for this thermometer is available and the magnetic field effect on this curve is unknown, temperature stabilization was performed at zero magnetic field by applying a constant power to the cryostat heater. The magnetic field was swept up and back down to zero, a check made that the temperature had not drifted during the field sweep, and the temperature then restabilized at another value. To avoid Joule heating and to keep the temperature deviation in the field small, a plastic sample-thermometer holder and small sweep rates for the magnetic field (1 T/min and -2T/min) were used. These procedures are one of the standard approaches used at the NHMFL for correct temperature measurements in high magnetic fields.

We have analysed the resistivity data on the basis that

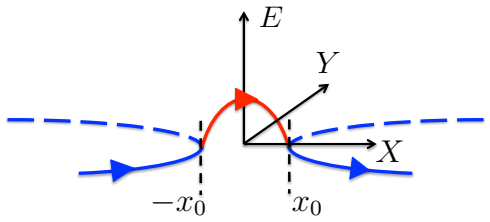

Figure 1. The path of the cyclotron orbit center, $\mathbf{R} = (X, Y)$, of a QP as it crosses a saddle point. The QP drifts along the classical trajectory, which encircles a local minimum of the impurity potential (left blue line). At the saddle point, it can either continue in the orbit (blue dashed line) or tunnel over the barrier and into the classical trajectory on the other side. The tunneling trajectory (red line) can be modelled within the WKB approach. It runs from $-x_0$ to x_0 the two points of closest approach. The effective Hamiltonian is that of an inverted parabola in one dimension, with momentum Y and coordinate X. The components of the cyclotron orbit coordinates, X and Y, are conjugate variables with $[X, Y] = il_q^2$ [1], where l_q is the QP magnetic length, and hence Y acts as the momentum to the position X.

the long range impurity potential, set up by the ionized donors, dominates the response in the quantum Hall regime. An indicator that this is the case, is given by the large value of the ratio of the lifetimes $\alpha = \tau_t/\tau_q = 78 \pm 2$ for our sample [2]. α is sometimes referred to as the Dingle ratio. Here τ_t is the transport lifetime. It is measured in zero magnetic field and characterizes the rate of momentum relaxation. The so-called quantum lifetime, τ_q, is deduced from the temperature and field dependence of the Shubnikov de Haas oscillations. It characterizes the rate at which dephasing occurs. A large value of τ_t/τ_q is taken to mean that a sample is dominated by the long-range impurity potential. While all scattering processes contribute to $1/\tau_q$, scattering off a long range potential involves predominantly small angle scattering that has a limited effect on momentum relaxation. The corresponding scattering rate, $1/\tau_t$, is smaller than $1/\tau_q$.

The slowly-varying backround potential, set up by the ionized donors, gives rise to compressible puddles of quasiparticles (QP) and quasiholes (QH), as indicated in Fig. 2 in the main text. The Coulomb interaction, it is assumed, ensures local equilibrium between excitations at the edges of these puddles and those at the center. An edge QP (QH) drifts along the equipotential lines surrounding the puddle, see Fig 1. At a saddle point it can cross the saddle point via a combination of thermal excitation and quantum tunneling. The probability of tunneling, as a function of the closest point of approach of the classical trajectory to the saddle point $\pm x_0$, was found in [1] to be given by $\mathcal{T}(x_0) = 1/(1 + \exp A)$ where $A = -\pi x_0^2/l_q^2$ with l_q the QP/QH magnetic length. This is the value predicted by the WKB approximation with $A = \int_{-x_0}^{x_0} Y \cdot X$, where Y is the momentum in the classically forbidden region.

The conductivity across the saddle is found after computing the net flow across the saddle and differentiating with respect to the chemical potential difference:

$$\sigma = \frac{(qe)^2}{h} \frac{1}{kT} \int_0^{\Delta_s} dE\, \mathcal{T}(E - E_s) e^{-E/kT}. \qquad (1)$$

Here $\mathcal{T}$ is written in terms of the energy of the QP excitation energy, E, which defines the point of closest approach, x_0, once a form for the potential is assumed. E_s is the height of the saddle, and Δ_s the gap [3]. We assume that the potential close to the saddle is given by $V(x, y) = (\Delta_s/2a^2)(-x^2 + y^2)$, where a is the typical width of the saddle (see Fig. 2 in the main text).

Each saddle point acts as an element in a network of resistors for QPs and as a separate element in a network for QHs [4]. The total conductance of the system is given by $2(W/L)\sigma$, where W/L is the effective aspect ratio of the network/sample with W its width and L its length. The computation of the resistance network relies on Dykhne's theorem [5], which states that, for a distribution of resistors in a network, for which the log of the resistance of the individual elements is symmetrically distributed about its mean, $\langle \log R \rangle$, the network resistance is $\exp\langle \log R \rangle$. We assume that the saddle point heights, E_{sp} and $E_{sh} = \delta_s - E_{sp}$, are evenly distributed about $\Delta_s/2$. Once tunnelling is included, $\log R$, is no longer strictly evenly distributed about its mean (as tunnelling increases the transition probability for $E_s < \Delta_s/2$ more than for $E_s > \Delta_s/2$). However, numerical studies of the corresponding resistor networks shows that the response changes only slightly from that obtained by assuming the validity of Dykhne's theorem. The deviations from a symmetric distribution are only significant far from the mean. These elements act essentially as short or open circuits and do not affect significantly the network resistance [6].

[1] H. A. Fertig and B. I. Halperin, Phys. Rev. B **36**, 7969 (1987).

[2] O. A. Mironov, A. H. A. Hassan, M. Uhlarz, S. Kiatgamolchai, A. Dobbie, R. J. H. Morris, J. E. Halpin, S. D. Rhead, P. Allred, M. Myronov, S. Gabani, I. B. Berkutov, and D. R. Leadley, Phys. Status Solidi C **11**, 61 (2014).

[3] N. d'Ambrumenil, B. I. Halperin, and R. H. Morf, Phys. Rev. Lett. **106**, 126804 (2011).

[4] D. G. Polyakov and B. I. Shklovskii, Phys. Rev. Lett. **73**, 1150 (1994).

[5] A. M. Dykhne, Sov. Phys. JETP **32**, 63 (1971).

[6] P. Asman, Unpublished, University of Warwick, (2015).